Integral ISS-Based Cascade Stabilization for Vectored-Thrust UAVs

Davide Invernizzi, Marco Lovera, Luca Zaccarian

Integral ISS-based cascade stabilization for vectored-thrust UAVs

Davide Invernizzi[1], Marco Lovera[1] and Luca Zaccarian[2]

***Abstract*—We address stabilization of vectored-thrust Unmanned Aerial Vehicles (UAVs): a challenging task due to the peculiar nonlinear underactuated dynamics. According to a well-established approach based on the selection of suitable error variables, the error dynamics is described as a pseudo cascade connection where the attitude subsystem indirectly stabilizes the position dynamics. Unlike existing works, we address stability of this cascade using integral Input to State Stability (iISS). With this extension it is possible to employ a quasi time-optimal control law to achieve global asymptotic stabilization of any desired position, thus improving the transient performance with respect to existing control designs. A simulation example shows the performance improvement in comparison with a nested saturations stabilizer.**

***Index Terms*—UAVs, integral ISS,**

I. Introduction

VECTORED-THRUST Unmanned Aerial Vehicles (UAVs) are platforms endowed with a propulsive system that can deliver a torque in any direction of the aircraft frame but a force only along a fixed axis: the thrust vector. Due to this underactuation, the position dynamics can be stabilized only through suitable attitude motions. There is a significant body of literature, well surveyed in [1], dealing with the stabilization problem for vectored-thrust UAVs as formulated in this paper, which is challenging also because it evolves on a nonlinear manifold corresponding to the set of rigid body motions. Early works on the subject date back to [2] and [3], while recent approaches are presented in [4], [5], [6].

The goal of this paper is to propose a control design which overcomes the limitations, in terms of transient performance, of modern strategies developed to globally stabilize the position of underactuated UAVs. In particular, the control designs proposed in [4], [5] as well as in our previous works [6], [7] ensure stability of the intrinsic cascade via a reduction approach [8] assessing the necessary property of "boundedness of solutions" by requiring the position stabilizer to possess Input to State Stabiliy (ISS) with respect to small inputs [9]. This small-signal ISS property is typically guaranteed by employing nested saturations-based stabilizers [5]: although very robust, this solution is known to yield poor transient performance [10].

Research supported in part by ANR via grant HANDY, number ANR-18-CE40-0010.

[1]Davide Invernizzi and Marco Lovera are with Dipartimento di Scienze e Tecnologie Aerospaziali, Politecnico di Milano, Via La Masa 34, 20156 Milano, Italy {davide.invernizzi, marco.lovera}@polimi.it

[2]Luca Zaccarian is with CNRS, LAAS, 7 avenue du colonel Roche, F-31400 Toulouse, France, Univ. de Toulouse, LAAS, F-31400 Toulouse, France, and Dipartimento di Ingegneria Industriale, University of Trento, Italy. zaccarian@laas.fr

In this paper, we propose a hierarchical control design that extends the class of allowable position stabilizers to solutions having less stringent robustness requirements, thereby allowing for a more aggressive behavior. In particular, after introducing the UAV dynamics and the control problem in Section II, we borrow tools from stability analysis of integral ISS cascades [11], [12], and we propose in Section III a control architecture inducing an autonomous pseudo-cascade structure of the closed-loop error dynamics while giving freedom in the selection of the attitude and position stabilizers and in the shape of the interconnection term, as long as they satisfy certain properties always ensuring boundedness of solutions. Then in Section IV, we select these three basic components using high performance strategies. In particular, we suggest using an exponential attitude stabilizer [13] and a Quasi Time-Optimal (QTO) stabilizer [14] and we prove that this choice makes the UAV position dynamics integral ISS. The QTO stabilizer is the prototypical example of aggressive solutions, achieving excellent transient performance, which cannot be included in existing designs, notably [4], [5], [6], since proving (the previously required) small-signal ISS property is hard if not impossible. A simulation example discussed in Section V highlights the advantage of the proposed solution with respect to a nested saturations approach in a scenario characterized by a significant initial configuration error.

Notation. $\mathbb{R}(\mathbb{R}_{>0},\mathbb{R}_{\geq 0})$ denotes the set of (positive, nonnegative) real numbers, $\mathbb{R}^n$ denotes the n-dimensional Euclidean space and $\mathbb{R}^{m\times n}$ the set of $m\times n$ real matrices. The canonical basis in $\mathbb{R}^n$ is denoted as $e_i := (0,\dots,1,\dots,0)$ for $i\in\{1,...,n\}$ and the identity matrix in $\mathbb{R}^{n\times n}$ is denoted as $I_n := [e_1\cdots e_i\cdots e_n]$. Given $x=(x_1,\dots,x_n)\in\mathbb{R}^n$, $\|x\| := \sqrt{x_1^2+\ldots+x_n^2}$ is the Euclidean norm while for a matrix $A\in\mathbb{R}^{n\times n}$, $\|A\|_F := \sqrt{\mathrm{tr}(A^TA)}$ is the Frobenius norm and $\mathrm{skew}(A) := \frac{A-A^T}{2}$ is the skew-symmetric part of A. The set $\mathrm{SO}(3) := \{R\in\mathbb{R}^{3\times 3} : R^TR = I_3, \det(R)=1\}$ denotes the third-order Special Orthogonal group while $\mathbb{S}^n := \{q\in\mathbb{R}^{n+1} : \|q\|=1\}$ denotes the n-dimensional unit sphere. where the normalized distance with respect to I_3, induced by the Frobenius norm, is denoted as $\|R\|_{\mathrm{SO}(3)} := \frac{1}{8}\|R-I_3\|_F = \sqrt{\frac{1}{4}\mathrm{tr}(I_3-R)}\in[0,1]$. Given $\omega\in\mathbb{R}^3$, the *hat* map $\hat{\cdot}:\mathbb{R}^3\to\mathfrak{so}(3) := \{\Omega\in\mathbb{R}^{3\times 3} : \Omega=-\Omega^T\}$ is such that $\hat{\omega}y = \omega\times y$, $\forall y\in\mathbb{R}^3$ and $\times$ represents the cross product in $\mathbb{R}^3$. The inverse of the *hat* map is the *vee* map, denoted as $(\cdot)^\vee:\mathfrak{so}(3)\to\mathbb{R}^3$. We use standard comparison functions from [15]: function $\alpha:\mathbb{R}_{\geq 0}\to\mathbb{R}_{\geq 0}$ is of class K if it is zero at zero, strictly increasing, and continuous. It is of class K_∞ if it is also unbounded. $\beta:\mathbb{R}_{\geq 0}\times\mathbb{R}_{\geq 0}\to\mathbb{R}_{\geq 0}$ is of class KL if it is of class K in the first argument and nonincreasing and converging to zero as its second argument tends to $+\infty$.

II. Dynamical model and control problem

The configuration of a UAV is globally and uniquely described by the pair $(R,x) \in \mathrm{SO}(3) \times \mathbb{R}^3$, where R and x are, respectively, the rotation matrix and the position vector of a body-fixed frame $\mathscr{F}_B = (O_B, \{b_1, b_2, b_3\})$ with respect to an inertial frame $\mathscr{F}_I = (O_I, \{i_1, i_2, i_3\})$. A reasonable model for control design is described by the following set of differential equations [1]:

$$\dot{x} = v \qquad m\dot{v} = -mge_3 + Rf_c \tag{1}$$

$$\dot{R} = R\hat{\omega} \qquad J\dot{\omega} = -\omega \times J\omega = -\hat{\omega}J\omega + \tau_c, \tag{2}$$

where $\omega \in \mathbb{R}^3$ is the *body* angular velocity, $v \in \mathbb{R}^3$ is the translational velocity of the center of mass, resolved in $\mathscr{F}_I$, $m \in \mathbb{R}_{>0}$ and $J = J^T \in \mathbb{R}^{3\times 3}_{>0}$ are the mass and the *body* inertia matrix of the UAV, respectively, and $g = 9.81\mathrm{m/s}^2$ represents the gravitational acceleration. Finally, $f_c \in \mathbb{R}^3$ is the control force and $\tau_c \in \mathbb{R}^3$ the control torque, both resolved in $\mathscr{F}_B$. The propulsive system of vectored-thrust UAVs allows to produce a (bounded) control force directed only along the positive direction of b_3, *i.e.*, the components of f_c in the body frame must satisfy

$$f_c = T_c e_3, \quad 0 < T_c \leq T_M \in \mathbb{R}_{>0}, \tag{3}$$

where T_c is the overall thrust that can be assigned by properly modulating the thrust delivered by each propeller. It is assumed that the control torque τ_c spans $\mathbb{R}^3$, *i.e.*, that the rotational dynamics (2) is *fully actuated*.

In this paper we exploit a cascade-based design for the attitude dynamics and consider $\omega_c := \omega$ as a control input, under the assumption that the attitude dynamics in equation (2) can be made sufficiently fast in tracking ω_c by a suitable selection of τ_c (for a discussion about this approximation, see [1]). In this case, the model for control design reduces to:

$$\dot{x} = v \tag{4}$$

$$m\dot{v} = -mge_3 + T_c R e_3 \tag{5}$$

$$\dot{R} = R\hat{\omega}_c \tag{6}$$

where the attitude motion (6) is independent of the translational one (4),(5). This structure is exploited in the hierarchical control strategy presented in the next section.

This work focuses on the stabilization of the underactuated model (4)-(6). According to this model, it is either possible to stabilize a desired attitude and altitude or a desired position and rotation about the gravity axis e_3. This paper addresses the latter problem under the following standard assumption.

Assumption 1: 1) the desired trajectory is a constant reference $(x_d, 0, R_d) \in \mathbb{R}^3 \times \mathbb{R}^3 \times \mathrm{SO}(3)$ such that $R_d e_3 = e_3$; 2) the maximum available thrust T_M is larger than the UAV weight, *i.e.*, $T_M > mg$; 3) the state of the system (x, v, R) is available for feedback.

While the first part of the assumption is necessary to account for the platform underactuation when constraint (3) is included in the dynamical model, the second part is necessary control authority requirement to have a solvable control problem. In view of Assumption 1, the control problem can be formally stated as follows.

Problem 1: Consider the dynamical model described by equations (4)-(6) and assume that the control thrust T_c is bounded as $0 < T_c \leq T_M$ for a strictly positive scalar T_M. Find a state feedback control law for $u := (T_c, \omega_c) \in (0, T_M] \times \mathbb{R}^3$ such that any constant set point $(x_d, 0, R_d) \in \mathbb{R}^3 \times \mathbb{R}^3 \times \mathrm{SO}(3)$ satisfying Assumption 1, is asymptotically stable.

III. Control design and stability analysis

This section is devoted to presenting the control design and the corresponding stability analysis. In [4], [5], [6] a small-signal ISS property was the basic requirement for the position stabilizer to ensure stability of the closed-loop system. Here we relax this requirement and enlarge the class of allowable position stabilizers towards solutions capable of superior performance. To this end, we invoke recent results on stabilization of nonlinear cascades, based on integral ISS arguments (see equation (24) below, and [11] for additional details about iISS). The formulation that we propose leaves the door open for different selections of stabilizers of the nominal position and attitude dynamics, therefore parametrizing a family of solutions to Problem 1.

A. Control law and closed-loop dynamics

We propose an attitude planner paradigm, similar to the one presented in our previous work [6], to tackle the system underactuation. Let us first introduce the stabilization error

$$e_x := x - x_d, \quad e_v := v, \quad R_e := R_p^T(e_x, e_v, R_d)R, \tag{7}$$

where $R_p : \mathbb{R}^3 \times \mathbb{R}^3 \times \mathrm{SO}(3) \to \mathrm{SO}(3)$ is the reference attitude provided by the attitude planner (see Figure 1) defined as:

$$R_p(e_x, e_v, R_d) := \left[\frac{b_{p_3} \times R_d e_1}{\|b_{p_3} \times R_d e_1\|} \times b_{p_3} \quad \frac{b_{p_3} \times R_d e_1}{\|b_{p_3} \times R_d e_1\|} \quad b_{p_3} \right], \tag{8}$$

where $b_{p_3} := \frac{f_d(e_x,e_v)}{\|f_d(e_x,e_v)\|}$ and

$$f_d(e_x, e_v) := \gamma_p(e_x, e_v) + mge_3 \tag{9}$$

is guaranteed to never vanish by design. Based on (8)-(9) we select the inputs of dynamics (4)-(6) as

$$T_c = c(R_e) e_3^T R_p^T(e_x, e_v, R_d) f_d(e_x, e_v) \tag{10}$$

$$\omega_c = \gamma_R(R_e) + R_e^T \omega_p(e_x, e_v, R_d), \tag{11}$$

where $\gamma_p : \mathbb{R}^3 \times \mathbb{R}^3 \to \mathbb{R}^3$ and $\gamma_R : \mathrm{SO}(3) \to \mathbb{R}^3$ are static state feedback stabilizers, $c(\cdot)$ is an interconnection term, to be selected, and $\omega_p(e_x, e_v, R_d) := (R_p^T \dot{R}_p)^\vee$ is the angular velocity reference computed by the attitude planner (see [6], [7] for details).

Proposition 1: Consider dynamics (4)-(6) with the stabilization errors in (7) and controller (10)-(11). If $f_d(e_x, e_v) \neq 0$ $\forall (e_x, e_v) \in \mathbb{R}^6$, then the closed-loop dynamics reads:

$$\dot{e}_x = e_v \tag{12}$$

$$m\dot{e}_v = \gamma_p(e_x, e_v) + \Delta R(R_e, e_x, e_v, R_d) f_d(e_x, e_v) \tag{13}$$

$$\dot{R}_e = R_e \hat{\gamma}_R(R_e) \tag{14}$$

where

$$\Delta R(R_e, e_x, e_v, R_d) := c(R_e) R_p(e_x, e_v, R_d) R_e R_p^T(e_x, e_v, R_d) - I_3. \tag{15}$$

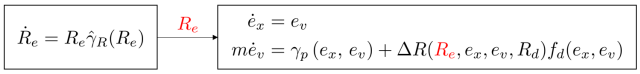

Figure 1. Cascade structure of the error dynamics (equations (12)-(14)).

Proof. We start by inspecting the position dynamics in (4), (5) and refer to the position and velocity errors defined in (7). By taking their time derivative along (4)-(5), we get

$$\dot{e}_x = e_v \tag{16}$$
$$m\dot{e}_v = m(\dot{v} - \dot{v}_d) = -mge_3 + T_c R e_3. \tag{17}$$

By noting that $T_c e_3 = c(R_e) R_p^T f_d$, equation (17) becomes

$$m\dot{e}_v = -mge_3 + c(R_e) R R_p^T f_d. \tag{18}$$

The velocity error dynamics can be further rewritten as

$$\begin{aligned} m\dot{e}_v &= -mge_3 + c(R_e) R_p R_p^T R R_p^T f_d \\ &= -mge_3 + c(R_e) R_p R_e R_p^T f_d. \end{aligned} \tag{19}$$

Finally, adding and subtracting f_d from equation (9), we get

$$m\dot{e}_v = \gamma_p(e_x, e_v) + \left(c(R_e) R_p R_e R_p^T - I_3\right) f_d, \tag{20}$$

corresponding to $\Delta R(R_e, e_x, e_v, R_d)$ in (15). For the attitude dynamics, using the definition of R_e in (7), we get:

$$\dot{R}_e = \dot{R}_p^T R + R_p \dot{R} = -\hat{\omega}_p R_p^T R + R_p^T R \hat{\omega} \tag{21}$$
$$= R_p^T R (\hat{\omega}_c - (R_p R)^T \hat{\omega}_p R_p^T R) = R_e(\hat{\omega}_c - R_e^T \hat{\omega}_p R_e). \tag{22}$$

Finally, using controller (11) and using property $(R_e \omega_p)^\wedge = R_e^T \hat{\omega}_p R_e$, the closed-loop (12)-(14) is obtained. □

Remark 1: The position error (12)-(13) is affected by the attitude error through the term $\Delta R f_d$, which weighs the mismatch between the desired force f_d in (9) and the control force resolved in $\mathcal{F}_I$, *i.e.*, $R f_c$. As shown in [6], the interconnection function $c(\cdot)$ in (15) helps improving the transient performance by shaping the mismatch term. ⌟

B. Cascade stability analysis and stabilizers

Control law (10)-(11) induces a pseudo cascade structure of the closed-loop dynamics (Figure 1) while leaving freedom in the selection of the attitude and position stabilizers $\gamma_R(\cdot)$ and $\gamma_p(\cdot,\cdot)$, as well as in the selection of the connection term ΔR, which depends upon the scaling function $c(\cdot)$. Clearly, their selection must guarantee asymptotic stabilization of the equilibrium $(R_e, e_x, e_v) = (I_3, 0, 0)$. The following definition [12] will be used to characterize the admissible iISS gains when the speed of convergence of the perturbing subsystem is exponential.

Definition 1: A function $\eta(\cdot)$ is said to be of class-H_I if it is of class-K and satisfies $\int_0^1 \frac{\eta(s)}{s} ds < \infty$.

The following result is a slightly modified version of [12, Corollary 2], adapted to our system evolving on $\mathbb{R}^6 \times \mathrm{SO}(3)$.

Lemma 1: Let $x \in \mathbb{R}^6$ and $R \in \mathrm{SO}(3)$ and consider the cascade $\dot{x} = f(x,R)$, $\dot{R} = Q(R)$ where $f : \mathbb{R}^6 \times \mathrm{SO}(3) \to \mathbb{R}^6$ and $Q : \mathrm{SO}(3) \to T\mathrm{SO}(3)$ are smooth vector fields with $f(0, I_3) = 0$ and $Q(I_3) = 0$. Suppose that the equilibrium $R = I_3$ is locally exponentially stable (LES) for $\dot{R} = Q(R)$, namely there exist c_R, $\lambda_R \in \mathbb{R}_{>0}$ and $\ell \in (0,1)$ such that $\|R(0)\|_{\mathrm{SO}(3)} \leq \ell$ implies

$$\|R(t)\|_{\mathrm{SO}(3)} \leq c_R \|R(0)\|_{\mathrm{SO}(3)} \exp(-\lambda_R t),\ t \geq 0. \tag{23}$$

If the dynamics $\dot{x} = f(x,R)$ is iISS with respect to input R with a class-H_I gain, namely, if there exist a class-K_∞ function $\alpha(\cdot)$, a class-KL function $\beta(\cdot)$, and a class-H_I gain $\eta(\cdot)$ such that, for all $t \geq 0$,

$$\alpha(\|x(t)\|) \leq \beta(\|x(0)\|, t) + \int_0^t \eta(\|R(\tau)\|_{\mathrm{SO}(3)}) d\tau, \tag{24}$$

then $(x,R) = (0, I_3)$ is locally asymptotically stable with domain of attraction including the set $\left\{(x,R) : x \in \mathbb{R}^6, R \in \mathrm{SO}(3), \|R\|_{\mathrm{SO}(3)} \leq \ell\right\}$.

Proof. The proof hinges upon the iISS property guaranteed by inequality (24). In particular, from (23) we have that $\|R(0)\|_{\mathrm{SO}(3)} \leq \ell$ implies

$$\begin{aligned} \int_0^\infty \eta(\|R(\tau)\|_{\mathrm{SO}(3)}) d\tau &\leq \int_0^\infty \eta\left(c_R \|R(0)\|_{\mathrm{SO}(3)} \exp(-\lambda_R \tau)\right) d\tau \\ &= \frac{1}{\lambda_R} \int_0^{c_R \|R(0)\|_{\mathrm{SO}(3)}} \frac{\eta(s)}{s} ds \end{aligned} \tag{25}$$

where we used $s := c_R \|R(0)\|_{\mathrm{SO}(3)} \exp(-\lambda_R \tau)$. Then, because $\eta(\cdot)$ is of class-H_I, the function

$$\nu(\bar{s}) := \frac{1}{\lambda_R} \int_0^{\bar{s}} \frac{\eta(s)}{s} ds \tag{26}$$

is well-defined for all $\bar{s} \in \mathbb{R}_{\geq 0}$ and it is of class-K because $\nu(0) = 0$ and $\frac{\eta(s)}{s} > 0$ for all $s > 0$. Thus, from property (24), we can write:

$$\alpha(\|x(t)\|) \leq \beta(\|x(0)\|, t) + \nu(c_R \|R(0)\|_{\mathrm{SO}(3)}). \tag{27}$$

This proves that all solutions are bounded. Furthermore, since $\int_0^\infty \eta(\|R(\tau)\|_{\mathrm{SO}(3)}) d\tau$ is bounded, (24) implies that $x(t) \to 0$ as $t \to \infty$ following the arguments in [11, Prop. 6]. □

System (12)-(14) can be written as in Lemma 1 by defining $e_p := (e_x, e_v) \in \mathbb{R}^6$ and $R := R_e \in \mathrm{SO}(3)$. Therefore, the stabilization of the cascade (12)-(14) is possible if one can provide a suitable attitude stabilizer $\gamma_R(\cdot)$ in (14) guaranteeing (local) exponential stability[1] of the equilibrium $R_e = I_3$, a position stabilizer $\gamma_p(\cdot,\cdot)$ and a scaling function $c(\cdot)$ for which the position error dynamics (12)-(13) is iISS with respect to input R_e in the sense of (24). In this spirit, we define the following properties.

Property 1: The attitude stabilizer $R_e \mapsto \gamma_R(R_e)$ is continuous and such that the equilibrium point $R_e = I_3$ is locally exponentially stable for (6) with domain of attraction containing $\left\{R \in \mathrm{SO}(3) : \|R\|_{\mathrm{SO}(3)} \leq \ell\right\}$ for some $\ell \in (0,1)$.

Property 2: The position stabilizer $(e_x, e_v) \mapsto \gamma_p(e_x, e_v)$ is continuously differentiable and the scaling function $R_e \mapsto c(R_e)$ is continuous and they are such that

[1] Due to topological obstructions of SO(3), only a local exponential result can be achieved with continuous static state feedback [16]. Nonetheless, it can be shown that the basin of attraction can be extended up to the set $\left\{R \in \mathrm{SO}(3) : \|R\|_{\mathrm{SO}(3)} < 1\right\}$ which does not contain only rotations about any axis of πrad away from I_3. Moreover, the results can be extended to global ones by using hybrid stabilizers [17].

1) there exist class-K_∞ and KL functions $\alpha(\cdot)$ and $\beta(\cdot)$ and a class-H_I gain $\eta(\cdot)$ such that the (e_x, e_v)-subsystem in equations (12), (13), (15) is iISS from R_e as in (24);
2) there exist saturation levels $M_i \in \mathbb{R}_{>0}$, $i \in \{1,2,3\}$, satisfying

$$M_3 < mg, \quad \sum_{i=1}^{3} M_i \leq T_M - mg \tag{28}$$

and such that the components of γ_p are bounded as $|\gamma_{p_i}(e_x, e_v)| \leq M_i \ \forall (e_x, e_v, i) \in \mathbb{R}^6 \times \{1,2,3\}$.

Remark 2: The second item in Property 2 and the continuous differentiability of $\gamma_p(\cdot,\cdot)$ are required in order to obtain a planner reference $R_p(e_x, e_v, R_d)$ as defined in equations (8)-(9) that is well-defined and C^1 $\forall (e_x, e_v, R_d) \in \mathbb{R}^3 \times \mathbb{R}^3 \times \mathrm{SO}(3)$ (see [6, Section IV-C] for additional details). ⌟

Based on the above properties and Lemma 1, the main result of the paper is then given by the following theorem.

Theorem 1: Consider the closed-loop system described by (4)-(6) controlled by (8)-(11). If $\gamma_R(\cdot), \gamma_p(\cdot,\cdot)$ and $c(\cdot)$ are selected according to Properties 1 and 2, then for any desired constant trajectory $(x_d, 0, R_d) \in \mathbb{R}^3 \times \mathbb{R}^3 \times \mathrm{SO}(3)$ satisfying Assumption 1, the control law (10)-(11) solves Problem 1, in particular the point $(e_x, e_v, R_e) = (0,0,I_3)$ is asymptotically stable with domain of attraction containing $\mathbb{R}^3 \times \mathbb{R}^3 \times \left\{R \in \mathrm{SO}(3) : \|R\|_{\mathrm{SO}(3)} \leq \ell\right\}$.

Proof. The proof follows the same steps as the proof of Lemma 1. Indeed, since the planner reference is C^1 and well-defined (see Remark 2), the control input ω_c in (11) is well-defined as well, and Proposition 1 ensures that the steps in Lemma 1 can be completed. Moreover, thanks to (28) and Assumption 1, the control force is bounded by T_M. □

IV. Sample Stabilizers Design

In this section we present a selection of the basic components of the control law, namely $\gamma_p(\cdot,\cdot)$, $\gamma_R(\cdot)$, $c(\cdot)$ and show that they satisfy Properties 1 and 2, thereby guaranteeing the applicability of Theorem 1. Specifically, we adopt a quasi time-optimal strategy for position stabilization, adapted from [14], which consists of a locally Lipschitz state feedback that behaves linearly in a neighborhood of the origin, but coincides with the time-optimal bang-bang feedback in the presence of large velocity errors. The QTO stabilizer is a representative candidate of aggressive solutions with excellent transient performance, but limited robustness properties: while we are not able to prove that the QTO enjoys a small-signal ISS property, which makes it unfit for existing strategies, we show that it enjoys integral ISS as in (24).

A. Attitude stabilization

The next proposition gives an example of an attitude stabilizer for which Property 1 is satisfied.

Proposition 2: Given $\gamma_R(R_e) := -\frac{k_R}{\sqrt{1+\mathrm{tr}(R_e)}}\mathrm{skew}(R_e)^\vee$, where $k_R \in \mathbb{R}_{>0}$ is a scalar gain, Property 1 is satisfied for any $\ell \in (0,1)$. In particular, the (closed-loop) trajectories of (14) converge exponentially to $R_e = I_3$ for all initial conditions starting in set $S_R := \left\{R \in \mathrm{SO}(3) : \|R\|_{\mathrm{SO}(3)} < 1\right\}$.

Proof. The proof follows from Lyapunov arguments, by considering the candidate Lyapunov function $V_R(R_e) := k_R(2 - \sqrt{1+\mathrm{tr}(R_e)})$ which is quadratic in the error, namely, $k_R\|R_e\|^2_{\mathrm{SO}(3)} \leq V_R(R_e) \leq 2k_R\|R_e\|^2_{\mathrm{SO}(3)}$ (see [13, equation 12.4]), and continuously differentiable in S_R. Indeed, by taking its time derivative along the dynamics (14) and by exploiting the trace operator property $\mathrm{tr}(A\hat{y}) = \mathrm{tr}(\mathrm{skew}(A)\hat{y}) = -2(\mathrm{skew}(A)^\vee)^T y$, $A \in \mathbb{R}^{3\times 3}$, $y \in \mathbb{R}^3$, we get:

$$\begin{aligned}\dot{V}_R(R_e) &= -\tfrac{k_R}{2\sqrt{1+\mathrm{tr}(R_e)}}\mathrm{tr}(\dot{R}_e)) \underset{(14)}{=} -\tfrac{k_R}{2\sqrt{1+\mathrm{tr}(R_e)}}\mathrm{tr}(R_e\hat{\gamma}_R(R_e)) \\ &= -\tfrac{k_R}{2\sqrt{1+\mathrm{tr}(R_e)}}\mathrm{tr}\left(\mathrm{skew}(R_e)\hat{\gamma}_R(R_e)\right) \\ &= \tfrac{k_R(\mathrm{skew}(R_e)^\vee)^T}{\sqrt{1+\mathrm{tr}(R_e)}}\gamma_R(R_e) = -\|\gamma_R(R_e)\|^2, \end{aligned} \tag{29}$$

which is continuous and negative definite in S_R (note that $\gamma_R(R_e)$ is well-defined in S_R since $\mathrm{tr}(R) = -1 \Leftrightarrow \|R\|_{\mathrm{SO}(3)} = 1$). Furthermore, since it can be shown that $\|\gamma_R(R_e)\| = k_R\|R_e\|_{\mathrm{SO}(3)}$ $\forall R_e \in S_R$, equation (29) can be written as

$$\dot{V}_R(R_e) = -k_R^2\|R_e\|^2_{\mathrm{SO}(3)} \leq -\tfrac{k_R}{2}V_R(R_e) \ \forall R_e \in S_R. \tag{30}$$

If we take $R_e(0) \in S_{V_R} := \{R \in \mathrm{SO}(3) : V_R(R) < 2k_R\}$, $\mathrm{tr}(R_e(0)) \neq -1$ since $\mathrm{tr}(R_e) = -1 \Leftrightarrow V_R(R_e) = 2k_R$ and $V_R(R_e)$ is forced to decrease by continuity by virtue of (30) and $\gamma_R(R_e)$, in turn, is well-defined. Accordingly, for all initial conditions in S_{V_R}, the solutions of system (14) satisfy $V_R(R_e(t)) = V_R(R_e(0))\exp\left(-\frac{k_R}{2}t\right)$ $\forall t \geq 0$. It is worth remarking that as subsets, S_R and S_{V_R} are equal, and therefore S_R is positively invariant. Finally, since V_R is quadratic, it can be easily shown that $\|R_e(t)\|_{\mathrm{SO}(3)} \leq \sqrt{2}\|R_e(0)\|_{\mathrm{SO}(3)}\exp\left(\frac{-k_R}{4}t\right)$ $\forall t \geq 0$, for all initial conditions starting in S_R. Finally, Property 1 is satisfied since for any $\ell \in (0,1)$ we have that $\left\{R \in \mathrm{SO}(3) : \|R\|_{\mathrm{SO}(3)} \leq \ell\right\} \subseteq S_R$. □

Remark 3: The stabilizer used in Proposition 2 is only one among several possible alternatives. By exploiting the angle axis parametrization $\mathbb{S}^2 \times (-\pi, \pi) \ni (n, \theta) \mapsto R(n,\theta) \in \mathrm{SO}(3)$, it is readily seen that $\|\gamma_R(R_e(n,\theta))\| = k_R\sqrt{\frac{1-\cos(\theta)}{2}} \leq k_R$, which reveals that the proposed solution is bounded for any $R_e \in S_R$ and that $\lim_{\theta\to\pm\pi}\|\gamma_R\| = k_R$. For large attitude errors, this is more aggressive than the standard selection $\gamma_R^0(R_e) := k_R\mathrm{skew}(R_e)^\vee$ which has a vanishing magnitude for $\theta \to \pm\pi$, since $\|\gamma_R^0(R_e(n,\theta))\| = k_R|\sin(\theta)|$. For further details about this comparison see [13]. ⌟

B. Position stabilization

A smooth version of the quasi time-optimal stabilizer for saturated double integrators, originally proposed in [14], and also used in [18], is employed as the position stabilizer in a decoupled form $\gamma_p(e_x, e_v) = (\gamma_{p_1}(e_{x_1}, e_{v_1}), \gamma_{p_2}(e_{x_2}, e_{v_2}), \gamma_{p_3}(e_{x_3}, e_{v_3}))$:

$$\gamma_{p_i}(e_{x_i}, e_{v_i}) := -\sigma_{M_i}\left(k_{x_i}\left(e_{x_i} + e_{v_i}\mu\left(\frac{|e_{v_i}|}{2M_i}, \frac{k_{v_i}}{k_{x_i}}\right)\right)\right), \tag{31}$$

for $i \in \{1,2,3\}$, where $k_{x_i}, k_{v_i} \in \mathbb{R}_{>0}$ are scalar PD-like gains assigning the small-signal linear behavior, $\sigma_{M_i}(\cdot)$ denotes a

continuously differentiable version of the saturation function satisfying $\sigma_{M_i}(s)s > 0$ if $s \neq 0$, whose components σ_{M_i} are bounded away from zero for large values of s and are globally bounded by $|\sigma_{M_i}(s)| \leq M_i$ with $M_i \in \mathbb{R}_{>0}$ arbitrarily selected. Finally function $\mu(a,b) := \sqrt[n]{a^n + b^n}$, $a,b \in \mathbb{R}_{\leq 0}$, for some $n \geq 1$ is a smooth approximation of the maximum of two non-negative scalars. The next proposition establishes iISS from the attitude error input of the arising position closed-loop (12), (13), (31).

Proposition 3: Consider the selection $c(R_e) := 1$ and the QTO position stabilizer (31). Then, Property 2 is satisfied.

Proof. The proof is based on [12, Lemma 1] establishing iISS if there exists a C^1, positive definite and radially unbounded function $V(e_x,e_v)$ and a class-H_I function $\eta(\cdot)$ such that $\dot{V}(e_x,e_v) \leq \eta(\|R_e\|_{\mathrm{SO}(3)})$. To this end, consider the following Lyapunov candidate for the unperturbed system, proposed in [18]:

$$V_p(e_x,e_v) := \tfrac{1}{2}m\sum_{i=1}^{3} k_{x_i} e_{v_i}^2 + \sum_{i=1}^{3}\int_0^{u_i} \sigma_{M_i}(s)ds, \qquad (32)$$

which is positive definite and radially unbounded from the stated sector properties of σ_{M_i}. Applying [15, Lem. 4.3] and using the structure of the first term of V_p, there exist class-K_∞ functions $\alpha_m(\cdot), \alpha_M(\cdot)$ and a scalar $c_v \in \mathbb{R}_{>0}$ such that

$$c_v\|e_v\|^2 + \alpha_m(\|e_x\|) \leq V_p(e_x,e_v) \leq \alpha_M(\|e_p\|), \qquad (33)$$

where we denoted $e_p := (e_x,e_v)$. By straightforward derivations we first obtain

$$\frac{\partial V_p(e_p)}{\partial e_{x_i}} = -k_{x_i}\sigma_{M_i}(u_i) \qquad (34)$$

$$\frac{\partial V_p(e_p)}{\partial e_{v_i}} = mk_{x_i}e_{v_i} - k_{x_i}\sigma_{M_i}(u_i)\left(\mu_i + \frac{\partial \mu_i}{\partial e_{v_i}}e_{v_i}\right) \qquad (35)$$

where we used the shortcut notation $\mu_i := \mu\left(\frac{|e_{v_i}|}{2M_i}, \frac{k_{v_i}}{k_{x_i}}\right)$. Using $\mu_i \geq 0$ and $\frac{\partial \mu_i}{\partial e_{v_i}}e_{v_i} \geq 0$, the time derivative of V_p along the unperturbed dynamics (12), (13), (31) (namely $\Delta R f_d = 0$) satisfies

$$\dot{V}_p(e_x,e_v) = -\frac{1}{m}\sum_{i=1}^{3} k_{x_i}\left(\mu_i + \frac{\partial \mu_i}{\partial e_{v_i}}e_{v_i}\right)\sigma_{M_i}^2(u_i) \leq 0. \qquad (36)$$

The function μ_i is the $n-$norm of the vector $\left[\frac{|e_{v_i}|}{2M_i} \ \frac{k_{v_i}}{k_{x_i}}\right]^T$, for which one has the bound $\mu_i \leq \frac{|e_{v_i}|}{2M_i} + \frac{k_{v_i}}{k_{x_i}}$ and, by exploiting homogeneity, the same bound can be shown to hold also for $\frac{\partial \mu_i}{\partial e_{v_i}}e_{v_i}$. As a consequence, using the bounds and gradients in (33)-(35), for any $r > 0$, we may establish the upper bound:

$$\|e_p\| \geq r \Rightarrow \frac{\|\nabla_{e_p}V_p(e_p)\|}{V_p(e_p)} \leq \frac{c_1 + c_2\|e_v\|}{c_v\|e_v\|^2 + \alpha_m(r)} \leq c_3, \qquad (37)$$

for some scalars $c_1, c_2 \in \mathbb{R}_{>0}$, and $c_3 \in \mathbb{R}_{>0}$ possibly growing unbounded as r approaches zero. Inspired by (37), let us now define a C^1, positive definite and radially unbounded function

$$V(e_x,e_v) := \begin{cases} \ln(V_p(e_x,e_v)) & \text{if } V_p(e_x,e_v) > \mathrm{e} \\ \frac{1}{\mathrm{e}}V_p(e_x,e_v) & \text{if } V_p(e_x,e_v) \leq \mathrm{e} \end{cases} \qquad (38)$$

where e denotes Euler's number. Using (37) and the fact that the gradient of V_p is bounded in any compact set $\|e_p\| \leq r$, we obtain $\|\nabla V(e_p)\| \leq c_4$ for some $c_4 \in \mathbb{R}_{>0}$. Combining this bound with the complementary one in (37), inspecting the perturbed dynamics (12), (13), (31) and exploiting the unperturbed bound (36), we may write

$$\dot{V}(e_p) \leq \max(c_3,c_4)\,\|\Delta R(R_e,e_x,e_v,R_d)f_d(e_x,e_v)\|, \qquad (39)$$

where we may use $\|\Delta R f_d\|$ as a shortcut for the right hand side interconnection term in (13). Consider now the chain of inequalities $\|\Delta R f_d\| \leq \|\Delta R\|\|f_d\| \leq \|\Delta R\|_F\|f_d\|$. Then, since $\|\Delta R(R_e)\|_F = \|R_p^T R_e R_p - I_3\|_F = \sqrt{6 - 2\mathrm{tr}(R_e)} \leq 2\sqrt{2}\|R_e\|_{\mathrm{SO}(3)}$ (by exploiting the definition of the Frobenius norm, the trace operator properties and the inequality $-1 \leq \mathrm{tr}(A) \leq 3$ for any $A \in \mathrm{SO}(3)$ [7, eqn. (86)]) and since $\|f_d\| = \|\gamma_p(e_x,e_v) + mge_3\| \leq \sum_{i=1}^3 M_i + mg \leq T_M$ (by selecting $\sum_{i=1}^3 M_i \leq T_M - mg$ as per (28)), one gets:

$$\|\Delta R f_d\| \leq 2\sqrt{2}T_M\|R_e\|_{\mathrm{SO}(3)}. \qquad (40)$$

Finally, combining bounds (39), (40), we get $\dot{V}(e_p) \leq 2\sqrt{2}\max(c_3,c_4)\,T_M\|R_e\|_{\mathrm{SO}(3)} := \eta(\|R_e\|_{\mathrm{SO}(3)})$, where function $\eta(\cdot)$ is clearly of class-H_I, and we can apply [12, Lemma 1] to conclude that the $(e_x,e_v)-$subsystem is iISS with respect to input R_e and that the QTO stabilizer (31) satisfies Property 2. □

Remark 4: The selection $c(R_e) := 1$ corresponds to the choice adopted by most hierarchical strategies [4], [5]. Different solutions can be envisaged to improve performance, *e.g.*, $c(R_e) := \frac{\bar{c}-(1-e_3^T R_e e_3))}{\bar{c}}$, $\bar{c} > 2$, which guarantees reduced position overshoot for large initial attitude errors (see Remark 1 and [6, Section VI-C]). With this choice, it can be shown that the proof of Proposition 3 still works. ⌟

V. Simulation results

We present a simulation example to assess the performance of the proposed control law (10)-(11) when the attitude and position stabilizers are selected as in Propositions 2 and 3. We also compare the performance obtained with a nested saturations-based stabilizer, which is one of the most common solutions in the recent literature [5], [6], [4] to globally stabilize the position dynamics of UAVs. To better highlight the differences, we refer to ideal conditions in which the UAV is described by the control model (4)-(6). The considered UAV has mass $m = 1$kg and can deliver a maximum thrust of $T_M = 40$N. The gain of the attitude stabilizer $\gamma_R(\cdot)$ used in Proposition 2 is selected as $k_R = 40$. For the QTO stabilizer (31), the gains can be freely chosen to have a desired behavior in unsaturated conditions and are set to $k_{v_i} = 9$, $k_{x_i} = \frac{k_{v_i}^2}{4}$ (critical damping). The saturation levels are set to $M_i = 9$ for $i \in \{1,2,3\}$ so as to ensure the validity of (28). The nested saturations stabilizer used for comparison is the one employed in [5]:

$$\gamma_p(e_x,e_v) := -\lambda_2\sigma_1\left(\frac{k_2}{\lambda_2}\left(e_v + \lambda_1\sigma_1\left(\frac{k_1}{\lambda_1}e_x\right)\right)\right) \qquad (41)$$

where the gains are set to $k_1 = 0.06, k_2 = 9$ and the saturation levels to $\lambda_1 = 5, \lambda_2 = 9$. While we have used the same outer saturation level $\lambda_2 \equiv M_i$ and damping gain $k_2 \equiv k_{v_i}$ of

the QTO stabilizer, we had to follow the guidelines of [5, Prop. 1] in selecting k_1 and λ_1, to guarantee the small-signal ISS property. Different selections of the control parameters could be considered but the constraints among them [5, eq. (26)] ultimately pose an intrinsic limitation to the achievable performance possibly caused by the strong ISS robustness property. As already mentioned, this is a common issue shared by nested saturations-based stabilizers [10].

The initial state of the UAV is $x(0) = (4,4,4)$m, $v(0) = (10,0,0)$m/s and $R(0) = I_3 + \sin(179.9^\circ)\hat{e}_1 + (1 - \cos(179.9^\circ)\hat{e}_1^2)$, which corresponds to an upside-down configuration with a significantly misplaced position with respect to the desired hovering position $x_d(0) = (0,0,1)$m, $R_d = I_3$. The attitude tracking performance is illustrated in Figure 2 (top) for both controllers. Since the same control law is used for attitude stabilization, the same attitude transient is achieved. On the contrary, the position errors are characterized by a quite different behavior. The aggressive nature of the QTO stabilizer results in an impressively faster response (see Figure 2 (bottom)). This desirable aggressive behavior is confirmed by inspecting Figure 3, where the thrust and the magnitude of the commanded angular velocity are depicted.

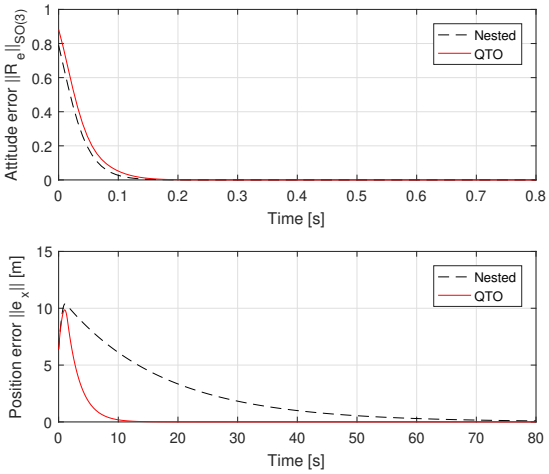

Figure 2. Stabilization errors: attitude $\|R_e\|_{\mathrm{SO}(3)}$ (top) and position $\|e_x\|$.

VI. Conclusions

The stabilization problem for vectored-thrust UAVs has been addressed using an inner-outer loop paradigm and integral ISS tools to analyze the arising pseudo cascade. This allows one to employ stabilizers with superior performance with respect to existing strategies while guaranteeing the same basin of attraction. Our stabilization results can be extended to trajectory tracking following the approach in [6], which should allow tracking in cluttered environments via suitable planners.

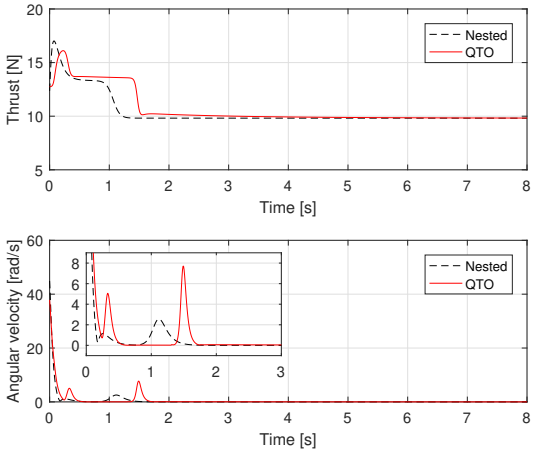

Figure 3. Control inputs: thrust T_c (top) and angular velocity $\|\omega_c\|$.

References

[1] M.-D. Hua, T. Hamel, P. Morin, and C. Samson, "Introduction to feedback control of underactuated VTOL vehicles: A review of basic control design ideas and principles," *IEEE Control Systems*, vol. 33, no. 1, pp. 61–75, 2013.

[2] E. Frazzoli, M. Dehleh, and E. Feron, "Trajectory tracking control design for autonomous helicopters using a backstepping algorithm," in *Proceedings of the American control conference*, vol. 6, 2000, pp. 4102–4107.

[3] T. Hamel, R. Mahony, R. Lozano, and J. Ostrowski, "Dynamic modelling and configuration stabilization for an x4-flyer." *IFAC Proceedings Volumes*, vol. 35, no. 1, pp. 217–222, 2002.

[4] A. Roza and M. Maggiore, "A class of position controllers for underactuated VTOL vehicles," *IEEE Transactions on Automatic Control*, vol. 59, no. 9, pp. 2580–2585, 2014.

[5] R. Naldi, M. Furci, R. G. Sanfelice, and L. Marconi, "Robust global trajectory tracking for underactuated VTOL aerial vehicles using inner-outer loop control paradigms," *IEEE Transactions on Automatic Control*, vol. 62, no. 1, pp. 97–112, 2017.

[6] D. Invernizzi, M. Lovera, and L. Zaccarian, "Geometric trajectory tracking with attitude planner for vectored-thrust VTOL UAVs," in *American Control Conference*, Milwaukee (WI), USA, Jul. 2018.

[7] ——, "Dynamic attitude planning for trajectory tracking in underactuated UAVs," *arXiv:1810.04494*, 2018.

[8] M. Maggiore, M. Sassano, and L. Zaccarian, "Reduction theorems for hybrid dynamical systems," *IEEE Transactions on Automatic Control*, 2019, to appear.

[9] A. Chaillet, D. Angeli, and H. Ito, "Combining iISS and ISS with respect to small inputs: the strong iISS property," *IEEE Transactions on Automatic Control*, vol. 59, no. 9, pp. 2518–2524, Sep. 2014.

[10] N. Marchand and A. Hably, "Global stabilization of multiple integrators with bounded controls," *Automatica*, vol. 41, no. 12, pp. 2147–2152, 2005.

[11] E. D. Sontag, "Comments on integral variants of ISS," *Systems & Control Letters*, vol. 34, no. 1, pp. 93–100, 1998.

[12] M. Arcak, D. Angeli, and E. Sontag, "A unifying integral ISS framework for stability of nonlinear cascades," *SIAM Journal on Control and Optimization*, vol. 40, no. 6, pp. 1888–1904, 2002.

[13] T. Lee, "Exponential stability of an attitude tracking control system on so (3) for large-angle rotational maneuvers," *Systems & Control Letters*, vol. 61, no. 1, pp. 231–237, 2012.

[14] F. Forni, S. Galeani, and L. Zaccarian, "A family of global stabilizers for quasi-optimal control of planar linear saturated systems," *IEEE Transactions on Automatic Control*, vol. 55, no. 5, pp. 1175–1180, May 2010.

[15] H. K. Khalil, *Nonlinear systems, 3rd Edition*. Prentice-Hall, 2002.

[16] D. E. Koditschek, "The Application of Total Energy as a Lyapunov Function for Mechanical Control Systems," *J. E. Marsden, P. S. Krishnaprasad and J. C. Simo (Eds) Dynamics and Control of Multi Body Systems*, vol. 97, pp. 131–157, February 1989.

[17] C. G. Mayhew, R. G. Sanfelice, and A. R. Teel, "Quaternion-based hybrid control for robust global attitude tracking," *IEEE Transactions on Automatic Control*, vol. 56, no. 11, pp. 2555–2566, Nov 2011.

[18] M. Andreetto, D. Fontanelli, and L. Zaccarian, "Quasi time-optimal hybrid trajectory tracking of an n-dimensional saturated double integrator," in *Proceedings of IEEE Conference on Control Applications (CCA)*, 2016, pp. 550–555.